N.A. DAVIDENKO, G.V. KUZNETSOV, YU.S. MILOVANOV

Taras Shevchenko National University of Kyiv, Institute of High Technologies
(64, Volodymyrs'ka Str., Kyiv 06001, Ukraine; e-mail: juri_milovanov@yahoo.com)

CADMIUM SULFIDE–POROUS SILICON NANOCOMPOSITE STRUCTURES

PACS 81.16.Rf

Optimum conditions for the formation of cadmium sulfide nanoparticles in a porous silicon matrix have been determined. The mechanisms of charge transfer in the formed heterostructures and their dependences on the porous layer properties and conditions of CdS nanoparticle synthesis have been studied. The spectral distribution and the intensity of photoluminescence are demonstrated to be governed by the concentration and the size of synthesized CdS nanocrystallites, as well as the efficiency of radiation recombination at deep centers bound with defects.

K e y w o r d s: porous silicon, CdS nanoparticles

1. Introduction

Researches of nanostructured materials obtained by forming semiconductor clusters and nanoparticles or inserting them into porous matrices [1–3] comprise one of the challenging directions in modern micro-electronics. Porous silicon is a material, in which the dimensions and the topology of its pores can be widely varied, which substantially extends the scope of its application as a material for the matrix insulation, luminescent markers, *etc.* [4–6]. Matrices on the basis of porous silicon allow nanocomposites with diverse electronic, optical, photo-electric, and adsorption properties to be fabricated using rather simple and inexpensive technologies. The parameters of such nanocomposites can be easily varied by changing the chemical composition and dimensions of synthesized clusters and nanoparticles, as well as by controlling the technological processes of filling the matrix pores and the crystallization in them.

Composite structures with nanocrystallites of semiconducting metal sulfides incorporated into a porous silicon matrix are promising for their application in photo-electric and optoelectronic microelectronic devices. The synthesis of metal sulfide nanocrystals with a wide range of energy gap values allows the problems of broadening the spectral range of recombination radiation and enhancing the photosensitivity to be solved in the framework of the same technology. The earlier results testify to a high quantum efficiency of disperse heterostruc-

tures on the basis of metal sulfides and porous silicon [4, 7, 8].

A tendency to the formation of various defects – deviations from a stoichiometry, dislocations, grain boundaries – which results in a reduction of the degradation resistance of composite structures, is typical of sulfide compounds [9, 10]. The problem concerning the instability of electronic and optical properties of porous silicon as a result of oxidation processes, hydrogen effusion, and formation of dangling bonds remains important [11–14]. Those circumstances form the background of the enhanced interest to the creation of stabilizing coatings in the bulk of a porous silicon matrix. The development of methods for the formation of coatings on the basis of sulfide compounds, in particular, cadmium sulfide, which combine stabilizing properties with high-quality electrical and optical parameters of synthesized composites is rather a challenging task.

In this work, the electrophysical and optical properties of composite structures obtained by chemical surface deposition of cadmium sulfide nanoparticles in a porous silicon matrix [15] are studied. The method is based on reactions occurring in the layers of adsorbed ions and allows the region of chemical reaction and CdS nanoparticle deposition to be localized in pores of the silicon matrix.

2. Specimens and Experimental Technique

Layers of nanoporous silicon were created by anodizing the (100) wafer of single-crystalline *p*-silicon (a specific resistance of 4.5 $\Omega \cdot$ cm). The electrochemical etching of silicon wafers was carried out
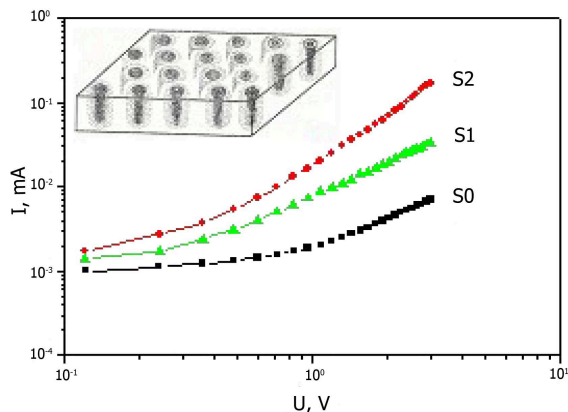
Fig. 1. Current-voltage characteristics of Ni–por-Si(CdS)–*p*-Si structures before (S0) and after (S1 and S2) CdS nanoparticle synthesis. The inset illustrates the model of nanostructured layer with cylindrically symmetric pores

in a mixture of fluoric acid and isopropyl alcohol, HF(48%):C_3H_7OH = 1:1, at a current density of 100 mA/cm^2. The thickness of the porous silicon layer was 10–15 μm, and its porosity 65–70%. The fabricated specimens were washed out in distilled water and dried in air.

For the formation of nanocomposite structures, we used the method of chemical surface deposition of sulfide compounds, which allowed us to localize the region, where the chemical reaction of nanoparticle formation occurred, to the volume of pores in the silicon matrix. The CdS compound synthesis was provided by the processes of irreversible ionic-exchange interaction in the aqueous solution of cadmium acetate $Cd(CH_3CO_2)_2$ (a source of Cd^{2+} cations) and sodium sulfide Na_2S (a source of S^{2-} anions). The presence of catalyzing vinyl monomers made it possible to form chemically stabilized CdS nanoparticles with a narrow spread of their dimensions on the substrate surface making no use of surface-active stabilizers. The surface tension of the solution gave rise to the minimization of the reaction mixture volume and its fixation on the substrate surface. The experimental specimens were classed into three groups. Group S0 included initial specimens before the CdS nanoparticle deposition; for specimens in group S1, the deposition time was $t_1 \approx 5 \div 6$ h; and, for specimens in group S2, the deposition time was $t_2 \approx 2t_1 \approx 10 \div 12$ h. CdS nanoparticles were synthesized at a temperature of 15–20 °C. At the final stage, the composite structures were washed out in distilled water and dried at 90 °C.

The morphological and structural characteristics of fabricated composite specimens were studied with the use of the raster electron microscopy method. Numerous pore holes were observed on the surface of initial porous silicon specimens, with a prevailing perpendicular pore orientation with respect to the (100) plane of the crystalline substrate. The CdS synthesis in pores and on the por-Si surfaces did not affect substantially the pore morphology and resulted in a uniform distribution of deposited nanoparticles with an average dimension of 3–5 nm. For longer deposition times (S2-specimens), a tendency for initially isolated nanosized CdS crystallites to agglomerate was observed.

To study the processes of electron transport, the both sides of a silicon wafer were covered with nickel contacts with the use of the electron-beam evaporation technique. The area of the upper contact was $S \approx 10^{-2}$ cm^2. The electrophysical and optical parameters of fabricated structures were researched at room temperature. The capacity-voltage characteristics were measured at the frequency $f = 1$ MHz by the bridge technique. The photoluminescence spectrum were excited with the help of nitrogen laser radiation at $\lambda = 337$ nm.

3. Results and Their Discussion

3.1. Electric parameters of synthesized structures

The fabricated Ni–por-Si(CdS)–*p*-Si structures were characterized by an insignificant asymmetry of their current-voltage characteristics, which testified to the dominating contribution of the intermediate porous layer to the total conductance of specimens [16, 17]. In Fig. 1, the current dependences on the direct voltage bias across the structure ("–" is applied to the Ni contact) are shown on the log-log scale. The formation of CdS nanoparticles in the pore volume of the silicon matrix results in a conductance growth, depending on the applied voltage.

The experimental current-voltage characteristics (I–V characteristics) can be described in the framework of the model of space-charge limited currents and supposing the presence of electron capture levels. In the initial region, the observed $I(U)$ dependence is close to the ohmic one and is governed by the concentration of thermally activated intrinsic equilibrium charge carriers in the porous layer. At

higher bias voltages ($U > 0.5 \div 0.7$ V), the growth in the concentration of injected electrons and their capture by deep traps result in the formation of a space charge, which is responsible for a typical square-law I–V dependence. For structures with incorporated CdS nanoparticles, the concentration n_t of charge carriers captured by traps can be evaluated by the formula [18]

$$n_t = \frac{\varepsilon_0 \varepsilon_{\mathrm{PS}} V_x}{e d_{\mathrm{PS}}^2}, \tag{1}$$

where V_x is the voltage of transition between the linear and square-law dependences, and d_{PS} and $\varepsilon_{\mathrm{PS}}$ are, respectively, the thickness and the dielectric permittivity of the porous layer experimentally determined from the capacity measurements for S2-specimens. The calculated values $n_t \sim 10^{18}$ cm^{-3} agree with known estimates for the trap concentration in semiconductor substances A^{2}B^6 with crystallite dimensions smaller than 100 nm [19].

The capacity-voltage characteristics ($f = 1$ MHz) measured before and after the CdS nanoparticle deposition had a shape typical of a MIS-structure with p-silicon substrate (Fig. 2). The process of empty pore filling with the sulfide phase characterized by a high dielectric permittivity ($\varepsilon_{\mathrm{CdS}} = 12$) gave rise to the capacitance growth for the porous layer and the whole structure.

The amount of the sulfide compound deposited in pores was determined with the use of the adsorption-capacitance porometry technique [20, 21]. In the general case, the capacitance of a porous silicon layer, C_{PS}, can be expressed as a sum of three components: the capacitance of the solid-state basis, C_{Si}, the capacitance of air-filled pores, C_{air}, and the capacitance of pores filled with the sulfide phase, C_{CdS}, i.e. $C_{\mathrm{PS}} = C_{\mathrm{Si}} + C_{\mathrm{air}} + C_{\mathrm{CdS}}$. In the framework of the model of a porous layer with cylindrically symmetric pores (see the inset in Fig. 1), the relative length of passing-through pores and the thickness of the solid-state silicon basis, d_{PS}, can be taken identical. The experimental value of the capacitance $C_{\mathrm{PS}} = \frac{\varepsilon_0 \varepsilon_{\mathrm{PS}} S}{d_{\mathrm{PS}}}$ is determined in the accumulation regime, when the total capacitance of the structure "surface–barrier" asymptotically approaches the geometrical capacitance of the high-resistance nanostructured layer, C_{PS}.

If there is no sulfide compound in the pores, we have $C_{\mathrm{PS}} = C_{\mathrm{Si}} + C_{\mathrm{air}}$, and, for the capacitance of
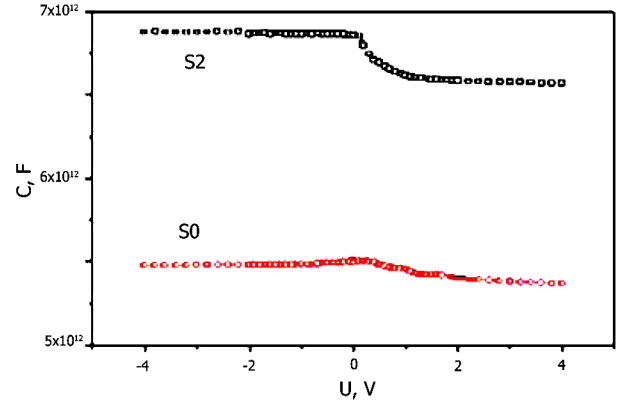

Fig. 2. Capacity-voltage characteristics of Ni–por-Si(CdS)–p-Si structures before (S0) and after (S2) CdS nanoparticle synthesis

porous silicon layer, we obtain

$$C_{\mathrm{PS}} = \frac{\varepsilon_0 \varepsilon_{\mathrm{PS}} S}{d_{\mathrm{PS}}} = \frac{\varepsilon_0 S}{d_{\mathrm{PS}}}[(1-\alpha)\varepsilon_{\mathrm{Si}} + \alpha \varepsilon_{\mathrm{air}}], \tag{2}$$

where $\alpha = S_{\mathrm{air}}/S$ is a parameter that characterizes the surface porosity of the layer, S is the area of the metal electrode, S_{air} is the area of pores under the electrode filled with air, and $\varepsilon_{\mathrm{Si}}$ and $\varepsilon_{\mathrm{air}}$ are the relative dielectric permittivities of the solid-state silicon basis and air, respectively. Provided the cylindrical pore model, the values of bulk and surface porosities coincide, which allows expression (2) to be used for the estimation of the porosity factor α.

To estimate the effective thickness d_{PS} of the porous layer, let us use the minimum values for the structure capacitance in the depletion regime, C_{min}, and consider the geometrical capacitance of the porous layer, C_{PS}, to be connected in series with the capacitance of the space charge region in silicon, $C_{\mathrm{SC\,min}}$,

$$\frac{1}{C_{\mathrm{min}}} = \frac{1}{C_{\mathrm{PS}}} + \frac{1}{C_{\mathrm{SCmin}}}. \tag{3}$$

The high-frequency capacitance C_{SCmin} reaches its minimum value in the strong-inversion regime,

$$C_{\mathrm{SCmin}} = \frac{(1-\alpha)\varepsilon_0 \varepsilon_{\mathrm{Si}} S}{W_m}, \tag{4}$$

where $W_m = 2\left(\frac{\varepsilon_0 \varepsilon_{\mathrm{Si}} kT \ln(N/n_i)}{e^2 N}\right)^{1/2}$ is the maximum width of the space charge region in silicon, N is a given impurity concentration, n_i is the concentration
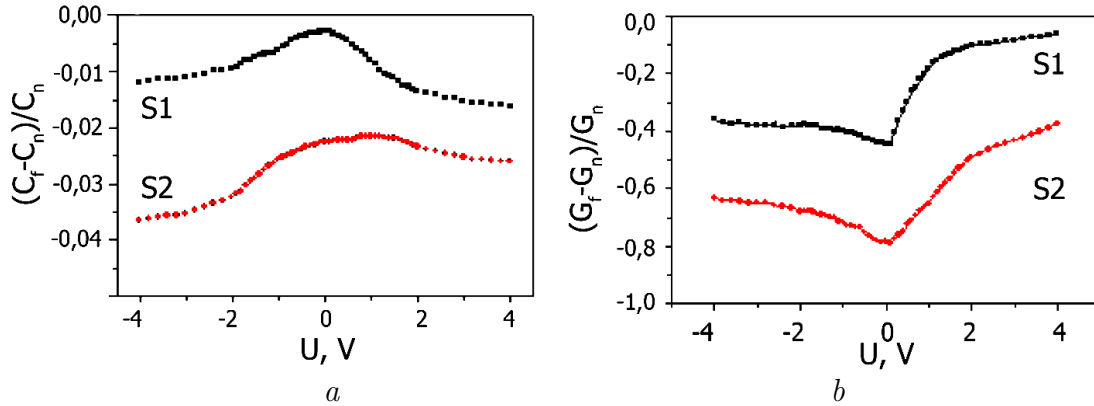
Fig. 3. Influence of the illumination on the capacitance (*a*) and conductance (*b*) characteristics of structures with synthesized CdS nanoparticles

of intrinsic charge carriers in silicon, k is the Boltzmann constant, T is the temperature, and e is the electron charge. Using the experimental values for C_{PS} and C_{min}, the value for the impurity concentration in silicon $N \approx 2 \times 10^{16}$ cm^{-3}, and Eqs. (1)–(3), we determine the porosity factor $\alpha = 60 \div 65\%$, the effective dielectric permeability $\varepsilon_{PS} = 4.8 \div 5.0$, and the porous silicon layer thickness $d_{PS} = 8 \div 10$ μm. The values obtained for the porosity factor of experimental specimens agree with those calculated from optical measurements [6].

For the structures with formed CdS nanolayers, it is necessary to take into account the capacitance of some pores filled with the sulfide compound characterized by the dielectric permittivity ε_{CdS}. If the sulfide phase volume equals V_{CdS}, expression (2) under adopted assumptions looks like

$$C_{PS(CdS)} =$$

$$= \frac{\varepsilon_0 S}{d_{PS}} \left[(1-\alpha)\varepsilon_{Si} + \left(\alpha - \frac{V_{CdS}}{d_{PS}S}\right)\varepsilon_{Air} + \frac{V_{CdS}}{d_{PS}\,S}\varepsilon_{CdS} \right]. \tag{5}$$

The difference between the values of porous layer capacitance before (Eq. (2)) and after (Eq. (5)) the cadmium sulfide nanoparticle deposition is determined by the expression

$$\Delta C = C_{PS(CdS)} - C_{PS} = \frac{\varepsilon_0 V_{CdS}}{d_{PS}^2}(\varepsilon_{CdS} - \varepsilon_{air}). \tag{6}$$

Estimations carried out according to formula (6) show that, for S2-specimens with the dielectric permittivity

$\varepsilon_{PS(CdS)} = 7.5 \div 8.0$, the fraction of pores filled with the sulfide phase does not exceed 15–20%.

In the Ni–por-Si(CdS)–*p*-Si heterostructures with synthesized cadmium sulfide nanoparticles in pores, illumination with light in the visible spectral range results in a reduction of their capacitance and conductance (Fig. 3). The dependences of the ac conductance ($f = 1$ MHz) on the illumination intensity correlate with the corresponding dependences for the constant current. This effect is similar to the stationary negative photoconductivity, which becomes lower than the dark value [22].

The variations in the conductance are governed by the processes of trap recharging that are invoked, when charge carriers absorb light. A considerable concentration of electron traps in cadmium sulfide nanocrystallites stimulates the almost complete capture of photoexcited electrons and leads to the creation of an extra motionless charge in the volume. In turn, it gives rise to a growth of photocurrent inertia and a reduction in the mobility of charge carriers owing to their additional scatterings by filled traps. A certain increase of the conductance with a growth of the applied voltage is associated with the increase in the concentration of free carriers (the trap release by the electric field).

3.2. Photoluminescence properties

The results of our researches concerning the photoluminescence properties of CdS–porous silicon structures are depicted in Fig. 4 for various durations of the CdS synthesis. The intensity of a photoluminescence signal from the initial porous silicon substrate is con-

siderably lower, by two to three orders of magnitude, in comparison with that registered from the structure with a synthesized CdS layer. Therefore, the measured spectra can be regarded as emitted by CdS nanoformations that were synthesized in the porous silicon layer.

The photoluminescence spectra of composite specimens CdS–pos-Si contain bands with maxima at $\lambda = 420 \div 430$, 550, 720, and 820 nm. Some maxima are a manifestation of various radiation recombination centers, the relative contribution of which depends on the solution composition, technology, and period of nanoparticle synthesis.

In the blue spectral interval, at $\lambda = 420$ nm, a peak of near-band-edge excitonic photoluminescence is observed, the intensity of which grows with the increase of the number of synthesized CdS nanoparticles (Fig. 4). The energy position of the short-wave band-edge luminescence band is governed by the processes of direct interband electron-hole recombination and is approximately equal to the energy gap width in CdS, $E_n = 2.9$ eV. The obtained values correlate with the results of researches dealing with the energy gap width in CdS nanocrystals and those calculated from the spectral dependence of the optical absorption coefficient [23]. The fundamental absorption edge is formed by optical transitions between the levels in the valence and conduction bands and depends on the size of CdS nanocrystals. For the estimation of the optical energy gap width and its dependence on the dimensions of CdS nanocrystallites, we may use the correlation expression [24]

$$E_n = E_0 + 0.71 \times \frac{\pi^2 \hbar^2}{2mR^2}, \tag{7}$$

where E_0 is the energy gap width in macrocrystalline CdS, E_n the same parameter in nanocrystalline CdS, m the mass of nanoparticle, and R its radius. Substituting the values $E_0 = 2.4$ eV and $E_n = 2.9$ eV for CdS nanoparticles (S1-specimens) into formula (7), we obtain, in the spherical approximation, the average particle size $R \approx 2 \div 3$ nm, which is in agreement with the results of measurements using the electron microscopy methods.

For specimens with a longer deposition time (S2-specimens), the edge luminescence band is shifted toward the short-wave range, which testifies to the
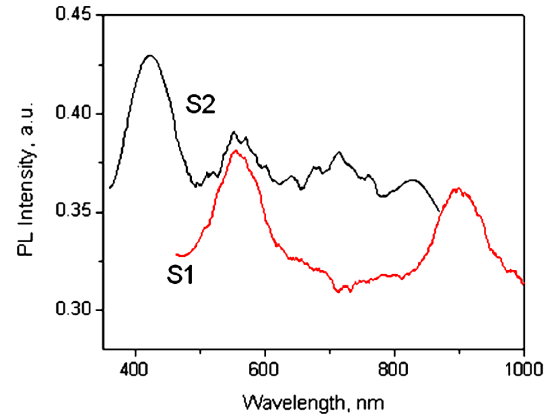

Fig. 4. Photoluminescence spectra of nanostructured layers por-Si(CdS) for the synthesis times $t_1 \approx 5 \div 6$ h (S1) and $t_2 \approx 2t_1 \approx 10 \div 12$ h (S2)

formation of fractions with smaller nanoparticle dimensions. Their appearance can be caused by features of the S^{2-} and Cd^{2+} ion deposition on the silicon matrix with a column pore structure. In the course of deposition, the free space in a pore diminishes until the pore walls start to interfere with the growth of CdS nanoparticles to their optimum size. Further, the particles are synthesized under conditions of the geometrical restriction imposed on the growth space and the limited supply of reacting components, which results in the formation of smaller nanocrystallites and an increase in the number of fractions with different nanocrystallite sizes [25].

The luminescence bands at longer wavelengths ($\lambda = 550$, 720, and 820 nm) are initiated by the recombination at impurity atoms and crystal lattice defects. We may suppose that, in undoped CdS nano- and macrocrystals, the luminescence processes are driven by intrinsic defects (mainly sulfur and cadmium vacancies) [26].

In nanocrystals, the effect of energy gap broadening induces a shift of photoluminescence bands toward higher energies. The most noticeably, this shift manifests itself for the peaks in the short-wave spectral range. In particular, for the orange band ($\lambda = 550$ nm), typical is the shift by about 0.2 eV, whereas, for the red one ($\lambda = 720$ nm), it does not exceed 0.05 eV. CdS nanocrystalline structures are characterized by larger band halfwidths (0.6–0.7 eV) in comparison with those for single-crystalline specimens (0.4 eV), which stems from the size spread
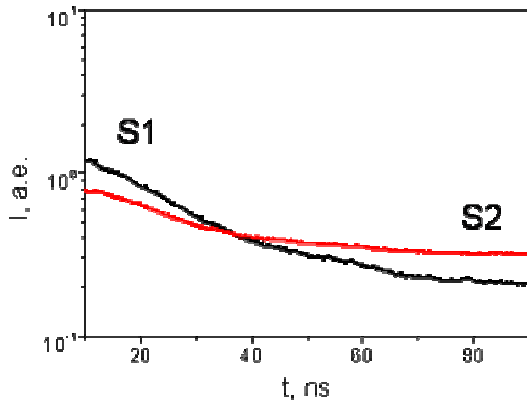
Fig. 5. Kinetic curves of the photoluminescence fading at $\lambda = 520$ nm

of nanoparticles. If the time of synthesis and, accordingly, the number of deposited CdS particles increase, the intensity of maxima at $\lambda = 520$ and 820 nm decreases, whereas the low-intensity band at $\lambda = 720$ nm grows (Fig. 4).

The origin of the band at $\lambda \approx 520$ nm is usually associated with luminescence centers related to sulfur vacancies V_S [26, 27]. Under the condition of S^{2-} ion deficiency, the electron-hole recombination at structural defects runs following the scheme

$$e^- + V_S \to V_S^-, \quad h^+ + V_S^- \to V_S + h\nu. \tag{8}$$
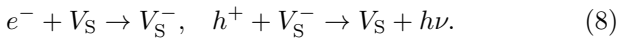
During the synthesis, the adsorption of excess sulfide ions results in a reduction of the concentration of corresponding radiative centers and a decrease of the intensity of the band at $\lambda \approx 520$ nm. Luminescence quenching after treating the specimen in the colloid solution testifies to a dominating localization of vacancies at the surface of synthesized nanoparticles.

The origin of the long-wave photoluminescence band at $\lambda = 720$ nm is associated with the presence of centers characterized by a deficiency of cadmium ions and the formation of the associative complex $V_{Cd}+V_S$ [27]. The electron-hole recombination at structural defects with engaging the cadmium vacancies is described by the relations

$$h^+ + V_{Cd} \to V_{Cd}^+, \quad e^- + V_{Cd}^+ \to V_{Cd} + h\nu. \tag{9}$$
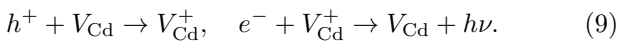
A relative reduction in the intensity of the band at $\lambda = 820$ nm for longer deposition times can be explained by changes in the stoichiometry and the formation of compensating acceptor V_{Cd} centers in the

crystals, which agrees with the literature data concerning the luminescence in cadmium sulfide macrocrystals.

The kinetic curves of photoluminescence quenching in CdS–por-Si specimens have a non-exponential character (Fig. 5). The total luminescence duration corresponds to the effective luminescence lifetime $\tau = 200 \div 300$ ns. The presence of particles with different sizes in the specimens gives rise to a wide set of photoluminescence lifetimes. The non-exponential character of the time dependences can be a result of the differences between the kinetics of radiative recombination processes in the bulk and at the surface of CdS nanocrystallites near the defects of various kinds – dislocations, heterointerfaces, *etc.* [28]. In this case, the appearance of an intensive wide radiation band with a short recession time can be explained by an emergence of radiative centers associated with the adsorption of sulfide compound molecules on the por-Si surface.

The analysis of the photocurrent relaxation kinetics for nanocomposite structures at a switched-on external electric field shows that the photoluminescence relaxation time does not depend on the influence of an external electric field on the specimen. This fact testifies to the presence of non-uniform internal electric fields and potential barriers, which affect the process of charge transfer in the course of photoexcitation [28]. Recombination barriers between low-resistance (with a high concentration of nonequilibrium major charge carriers) and high-resistance (with a high probability of charge carrier capture by recombination centers) regions give rise to the observable modifications in the relaxation kinetics in the porous silicon layers with incorporated cadmium sulfide nanoparticles. When the time of the chemical treatment of a specimen in the colloid solution increases, the migration of Cd^{2+} and S^{2-} ions over the surface of CdS nanoformations is activated, which can result in a reformation of the latter and a reconstruction of the system of recombination centers coupled with defects. At the initial stage, CdS nanoparticles are localized on the developed surface of the porous silicon layer with the penetration depth determined by the pore dimensions and topology. The formation of point defects occurs near the structural damages in the CdS crystal lattice, which affects the distribution of doping impurities, in par-

ticular, oxygen. As the pore filling degree grows, the nanoparticle fraction creates a fiber-like structure, which transforms the processes of defect formation at the sites, where interatomic bonds are weakened.

The aging effects manifest themselves insignificantly, being mainly associated with the centers of radiationless recombination of charge carriers that arise at the oxidation on the surface of nanocrystallites [3, 27]. Oxygen atoms are distributed non-uniformly over the nanocrystallite volume and form heterogeneous systems, which include aggregates with an increased or decreased oxygen concentration. The emergence of recombination barriers between the low- and high-resistance regions, which occurs owing to adsorbed oxygens, can promote the processes of photoexcited charge carrier capture by recombination centers.

4. Conclusions

On the basis of the chemical surface deposition method, the laboratory technique for synthesizing CdS nanoparticles in the bulk of a porous silicon matrix has been elaborated. The charge transfer in nanostructured layers of porous silicon was shown to depend on such factors as the pore morphology, chemical composition and size of incorporated particles, passivation of the porous matrix surface by impurity atoms, efficiency of charge carrier capture by surface traps, *etc.*. The photoluminescence spectrum of synthesized cadmium sulfide crystallites is determined by the radiative recombination at defect centers of two types, namely, sulfur vacancies V_{S} (the band at $\lambda_{\max} = 550$ nm) and associative complexes $V_{\mathrm{Cd}} + V_{\mathrm{S}}$ (the band at $\lambda_{\max} = 720$ nm), with the intensity ratio between those bands depending on the time and the technique of nanoparticle deposition. Wide opportunities to modify the pore size and the topology in the nanoporous silicon medium allow the problems dealing with the fabrication of nanocomposite structures of various types with required electric and optical properties to be solved.

1. *Ordered Porous Nanostructures and Applications,* edited by R.B. Wehrspohn (Springer, New York, 2005).
2. T. Serdiuk, V.A. Skryshevsky, I.I. Ivanov, and V.Lysenko, Mater. Lett. **65**, 2514 (2011).
3. E.B. Kaganovich, E.G. Manoilov, I.R. Basylyuk, and S.V. Svechnikov, Semiconductors **37**, 353 (2003).
4. A. Gokarna, N.R. Pavaskar, S.D. Sathaye, V. Ganesan, and S.V. Bhoraskar, J. Appl. Phys. **92**, 2118 (2002).
5. V. Lysenko, V. Onyskevych, O. Marty, V.A. Skryshevsky, Y. Chevolot, and C. Bru-Chevallier, Appl. Phys. Lett. **92**, 251910 (2008).
6. A.Y Karlach, G.V. Kuznetsov, S.V. Litvinenko, Y.S. Milovanov, and V.A. Skryshevsky, Semiconductors **44**, 1342 (2010).
7. N.V. Bondar and M.S. Brodyn, Ukr. J. Phys. **54**, 130 (2009).
8. N.V Deshmukh., T.M. Bhave, A.S. Ethiraj, S.R. Sainkar, V. Ganesan, S.V. Bhoraskar, and S.K. Kulkarni, Nanotechnology **12**, 290 (2001).
9. M.M. Vorontsova, N.V. Malushin, V.M. Skobeeva, and V.A. Smyntyna, Fotoelektronika **11**, 104 (2002).
10. G.S. Khrypunov, V.R. Kopach, A.V. Meriuts, R.V. Zaitsev, M.V. Kirichenko, and N.V. Deyneko, Semiconductors **45**, 1564 (2011).
11. V.A. Skryshevsky, Appl. Surf. Sci. **157**, 145 (2000).
12. B.M. Bulakh, N.E. Korsunska, L.Yu. Khomenkova, T.R. Stara, and M.K. Sheinkman, Semiconductors **40**, 614 (2006).
13. A. Korcala, W. Bała, A. Bratkowski, P. Borowski, and Z. Łukasiak, Opt. Mater. **28**, 143 (2006).
14. V.A. Skryshevsky, A. Laugier, V.I. Strikha, and V.A. Vikulov, Mater. Sci. Eng. B **40**, 54 (1996).
15. G.A. Ilchuk, V.V. Kusnezh, V.Yu. Rud, Yu.V. Rud, P.Yo. Shapowal, and R.Yu. Petrus, Semiconductors **44**, 335 (2010).
16. V.A. Vikulov, V.I. Strikha, V.A. Skryshevsky, S.S. Kilchitskaya, E. Souteyrand, and J.R. Martin, J. Phys. D **33**, 1957 (2000).
17. V. Strikha, V. Skryshevsky, V. Polishchuk, E. Souteyrand, and J.R. Martin, J. Porous Mater. **7**, 111 (2000).
18. A.A. Evtukh, Ukr. J. Phys. **54**, 308 (2009).
19. V.B. Lazarev, V.G. Krasov, and I.S. Shaplygin, *Electric Conductivity of Oxide Systems and Film Structures* (Nauka, Moscow, 1979) (in Russian).
20. I.V. Gavrilchenko, S.A. Diachenko, G.V. Kuznetsov, V.A. Skryshevsky, and Y.A. Pervak, Visn. Kyiv. Univ. Ser. Fiz. Mat. Nauky **8**, 41 (2005).
21. E.A. Tutov, A.Yu. Andryukov, and E.N. Bormontov, Semiconductors **35**, 850 (2001).
22. V.I. Gavrilenko, A.M. Grekhov, D.V. Korbutyak, and V.G. Litovchenko, *Optical Properties of Semiconductors: A Handbook* (Naukova Dumka, Kiev, 1987) (in Russian).

23. P. Zhang, P.S. Kim, and T.K. Sham, J. Appl. Phys. **91**, 6038 (2002).

24. L.E. Brus, Al. Efros, and T. Itoh, J. Lumin. **76**, 1 (1996).

25. Yu.Yu. Bacherikov, I.Z. Indutnyi, O.B. Okhrimenko, S.V. Optasyuk, P.Ye. Shepeliavyi, and V.V. Ponamarenko, Semiconductors **45**, 1235 (2011).

26. G. Ma, S. Tang, W. Sun, Z. Shen, W. Huang, and J. Shi, Phys. Lett. A **299**,581 (2002).

27. Y. Kanemitsua and A. Ishizumi, J. Lumin. **119–120**, 161 (2006).

28. V.N. Bondarev and P.V. Pikhitsa, Fiz. Tverd. Tela **43**, 2142 (2001).

М.О. Давиденко, Г.В. Кузнецов, Ю.С. Мілованов

ЕЛЕКТРОФІЗИЧНІ ТА ЛЮМІНЕСЦЕНТНІ
ВЛАСТИВОСТІ СИСТЕМ СУЛЬФІД
КАДМІЮ–ПОРИСТИЙ КРЕМНІЙ

Р е з ю м е

Визначено оптимальні умови формування нанокристалів сульфіду кадмію в матриці пористого кремнію. Досліджено механізми переносу носіїв заряду в сформованих гетероструктурах залежно від властивостей пористого шару та умов синтезу наночастинок CdS. Спектральний розподіл та інтенсивність фотолюмінесценції визначаються концентрацією та розмірами синтезованих наночастинок та ефективністю випромінювальної рекомбінації на зв'язаних з дефектами глибоких центрах.